Supporting Information submitted to Journal of Materials Chemistry A

Single-Cluster Polyoxometalate Catalysts via Modular Electrostatic Assembly on Cationic Covalent Organic Framework for Furfural Electroreduction

Peng Lei, [a] Weijie Geng, [a] Hui Zhang, [b] Peixuan Zhang, [a] Jie Li, [a] Jianxin Du, [c] Yingnan Chi,*[a] Changwen Hu [a]

[a] Key Laboratory of Cluster Science Ministry of Education, Beijing Key Laboratory of Photoelectronic/Electrophotonic Conversion Materials, School of Chemistry and Chemical Engineering, Beijing Institute of Technology, Beijing 100081, People's Republic of China.

[b] Analysis and Testing center, Soochow University, Suzhou, 215123, People's Republic of China.

[c] Analysis & Testing Center, Beijing Institute of Technology, Beijing, 100081, People's Republic of China.

E-mail: chiyingnan7887@bit.edu.cn

1. Material Synthetic Procedures

Synthesis of DNBP. Based on the reported procedure[1], 4,4'-bipyridine (5.00 g, 32.0 mmol, 1.00 eq) and 2,4-dinitrochlorobenzene (26.0 g,128 mmol, 4.00 eq) were mixed in dry acetonitrile (80.0 mL) and refluxed for 24 h. The resulting yellowish solution was cooled to room temperature and filtered. A bright yellow precipitate was obtained, then washed with anhydrous acetonitrile repeatedly until turning white. The product was dried in vacuum for 24 h. A white power was obtained, yield 46.3% based on 4,4'-bipyridine.

Synthesis of $[X_4(H_2O)_2(PW_9O_{34})_2]$ (X = Cu, Co, Ni; abbreviated as $X_4(PW_9)_2$). These three POMs were synthesized according to previous report[2-4]. For $Na_3K_7[Cu_4(H_2O)_2(PW_9O_{34})_2]\cdot 30H_2O$, solid $CuCl_2\cdot 2H_2O$ (0.62 g, 3.6 mmol) was dissolved in 12 mL of water. To this light blue solution was added slowly solid $[B\text{-}PW_9O_{34}]^{9-}$ (5.1 g, 1.8 mmol); the resulting mixture was vigorously stirred until a clear light green solution was obtained. Then 1 g of KCl was added, resulting in immediate precipitation of a pale green solid that was collected by centrifugation. The resulting precipitates were recrystallized by redissolving in 30 mL of warm water, and the slightly cloudy solution was centrifuged to remove any insoluble impurities. The clear green supernatant was left in a refrigerator at 4 °C for crystallization. After 2 days, pale green needle-shaped crystals were collected by filtration. The syntheses of $Co_4(PW_9)_2$ and $Ni_4(PW_9)_2$ were operated using the corresponding metallic salt $Co(OAc)_2\cdot 4H_2O$ or $Ni(OAc)_2$ in a similar process.

Synthesis of $[P_2W_{18}O_{62}]$ (abbreviated as P_2W_{18}). For $K_6[\alpha\text{-}P_2W_{18}O_{62}]\cdot 14H_2O$, 300 g of $Na_2WO_4\cdot 2H_2O$ is dissolved in 350 mL deionized water. 4 M HCl (250 mL, 1.00 mol) is added dropwise to the above clear solution followed by adding 4 M H_3PO_4 (250 mL, 1.00 mol). The resulting pale-yellow solution is subsequently refluxed for 24 h. After cooling down to room temperature, 150 g KCl is added into the resultant bright yellow solution under vigorous stirring to obtain the yellow precipitate. The yellow solution is filtered to remove insoluble impurities.

Finally, the solution is heated at 80 °C for 72 h and then proceeded to recrystallize in a 4 °C refrigerator.

Synthesis of $[Cu_2Na_2(PW_9O_{34})_2]$ (abbreviated as $Cu_2Na_2(PW_9)_2$). Based on the reported procedure,[5] $Na_2WO_4{\cdot}2H_2O$ (5 g, 15.2 mmol) and Na_2HPO_4 (0.24, 1.7 mmol) were dissolved in 100 mL H_2O followed by an addition of $Cu(NO_3)_2{\cdot}3H_2O$ (0.27 g, 1.1 mmol), resulting in a cloudy suspension. The pH was adjusted to 7.5 by dropwise addition of 6 mol L^{-1} HCl, and a light green solution formed. The solution was heated at 90 °C for 1 h and then was allowed to cool to room temperature. Powdered KCl (0.6 g, 8.0 mmol) was added, and the solution was left to slowly evaporate at room temperature to collect the needle crystals.

Synthesis of $[Cu(OH)_6W_6O_{18}]$ (abbreviated as CuW_6). CuW_6 was prepared based on the method reported in the literature.[6] Typically, $Na_2WO_4{\cdot}2H_2O$ (10.0 g) dissolved in water (80 mL) and heated to boiling. Then, $Cu(NO_3)_2$ (1.45 g) was slowly added and kept boiling for another 15 min (during the timely addition of water). At the end of the reaction, the same volume of hot water was added. After being kept at 80 °C in steam bath for 30 min, the products were collected though filtration and washed three times with deionized water.

Synthesis of $[PW_{11}O_{39}Cu(H_2O)]$ (abbreviated as $CuPW_{11}$). 10 mL aqueous solution of $H_3PW_{12}O_{40}$ (2.88 g, 1 mmol) was adjusted to 4.8 pH using a 6 mol L^{-1} NaOH solution, and heated to 90 °C with stirring. To this POM solution, $CuCl_2{\cdot}2H_2O$ (0.17 g, 3mol) dissolved in 5 mL water was added drop-wise, then refluxed for 1.5 h at 90 °C. This solution was hot filtered and solid KCl (2.0 g) was immediately added. The resulting greenish blue precipitates were filtered, dried at 60 °C. Most of the above synthesis methods have been reported multiple times.[7]

2. Experimental procedures

Cyclic voltammetry (CV) experiments. The CV tests were performed in an undivided three-electrode setup under ambient conditions, using the glassy carbon with/without the modification of electrocatalyst (such as PV, POM@PV) as the working electrode. The CV result was acquired with a scan rate of 50 mV s^{-1} and a scan range from 0 to -1.6 V (vs. Ag/AgCl). Multiple cycles (usually 3-10 cycles) were performed to obtain stable CV curves then record the same circle for comparison.

Linear sweep voltammetry (LSV). In an undivided three-electrode cell, LSV test employs carbon cloth as the working electrode to screen out catalysts that exhibit potential advantages in the FF electroreduction (using carbon cloth). The scan rate is 50 mV s^{-1} and the scan range from -0.1 to -1.6 V (vs. Ag/AgCl).

Constant voltage electrocatalytic reduction of FF. A constant potential (for a typical electroreduction of FF, -1.4 V vs. Ag/AgCl) was applied to the working electrode. The electrolysis was carried out and terminated when a total charge of 20 C was consumed. The current was monitored and recorded during the electrolysis process. Before the reaction, CV was also carried out in a H-type electrolytic cell to activate the catalyst.

Selectivity and Faradic efficiency calculation. Selectivity of furfuryl alcohol (FA Sele.) was defined as the percentage of the molar amount of generated FA relative to the total molar amount of consumed furfural (FF), directly reflecting the catalyst's ability to reduce FF to FA. The formula is given by:

$$FA\ Sele. = \frac{n_{FA,\ produced}}{n_{FF,\ consumed}} \times 100\%$$

Where $n_{FA,\ produced}$ is the molar amount of generated FA (in mmol), $n_{FF,\ comsumed}$ is the molar amount of consumed FF (in mmol).

For 2-hydroxymethylfuran (HDF) selectivity, the formula is analogous:

$$HDF\ Sele. = \frac{2 \times n_{HDF,\ produced}}{n_{FF,\ consumed}} \times 100\%$$

The Faradaic efficiency of FA (FA F.E.) is calculated as the ratio of the charge consumed for generating the target product FA to the total charge consumed during electrolysis. The FF electroreduction was set to terminate when the total charge reached 20 C, and the formula is:

$$FA\ F.E. = \frac{n_{FA,\ produced} \times 2 \times F}{Q_{total}} \times 100\%$$

Where $n_{FA,\ produced}$ is the molar amount of generated FA (in mmol), corresponding to a 2-electron reduction process of FF to FA, F is the Faraday constant (96485 C mol^{-1}), and Q_{total} = 20 C.

For HDF Faradaic efficiency, the formula is:

$$HDF\ F.E. = \frac{n_{HDF,\ produced} \times 2 \times F}{Q_{total}} \times 100\%$$

Electrochemical surface area measurement (ECSA). ECSA can be estimated by the capacitance of the double layer C_{dl}, based on the assumption that the two quantities are linearly proportional. The ECSA was evaluated within a potential window of 50-100 mV relative to the open-circuit potential of the electrochemical system, where no Faradaic processes occur. CV measurements were performed at multiple scan rates (20, 40, 60, 80, and 100 mV/s) to obtain current-potential curves. Subsequently, the capacitive current values at the midpoint of the selected potential window were extracted and the ECSA was derived from the slope of the capacitive current vs. scan rate plot.

Electrochemical impedance spectra (EIS). A glass carbon electrode served as the working electrode. The frequency range was set from 10000 Hz to 1 Hz. An AC perturbation signal with

an amplitude of 5 mV was applied at the open-circuit potential. For Bode plot phase-angle analysis, the potential was applied in sequence from -0.8 to -1.6 V vs. Ag/AgCl.

Radical scavenging experiments. Radical scavenger, 4-amino-2,2,6,6-tetramethylpiperidine-1-oxyl (4-NH_2-TEMPO, 0.50 mmol) was added into a standard electrocatalytic system and the electroreduction was performed under otherwise identical conditions. The reaction products were analyzed by liquid chromatogram and GC-MS (after 2mL dichloromethane extract). It investigated the involvement of reactive ketyl radicals in the electrocatalytic FF reduction reaction.

Partial current density of FA analysis. The partial current density of furfuryl alcohol (j_{FA}) was measured to quantify the catalytic activity of the catalyst toward FA formation during FF electroreduction, with the FF concentration as the variable parameter. For each FF concentration (5 mM, 10 mM, 20 mM, 50 mM, 100 mM, and 150 mM), constant-potential electrolysis was performed for a fixed duration of 20 minutes to ensure sufficient reaction progress. After electrolysis, the reaction solution was sampled. The partial current density j_{FA} was calculated using the formula:

$$j_{FA} = \frac{n_{FA,\ produced} \times 2 \times F}{t \times A}$$

Where $n_{FA,\ produced}$ is the molar amount of generated FA (in μmol), corresponding to a 2-electron reduction process of FF to FA, F is the Faraday constant (96485 C mol^{-1}), t is the electrolysis time (fixed at 1200 s), A is the area of working electrode (1×1 cm^2).

Experiment of quaternary ammonium cation modifying electrode. In a standard electrocatalytic system, bromide salts of four quaternary ammonium cations, namely tetramethylammonium (Me_4N^+, 0.2 mmol), tetraethylammonium (Et_4N^+, 0.2 mmol), tetrapropylammonium (Pr_4N^+, 0.2 mmol), and tetrabutylammonium (Bu_4N^+, 0.2 mmol/0.4 mmol), were added. After stirring to dissolve them, a voltage of -0.2 V was applied for 10

minutes to promote the aggregation and surface modification of quaternary ammonium cations on the working electrode. Subsequently, a standard electroreduction of FF was performed.

3. Supplementary experimental results

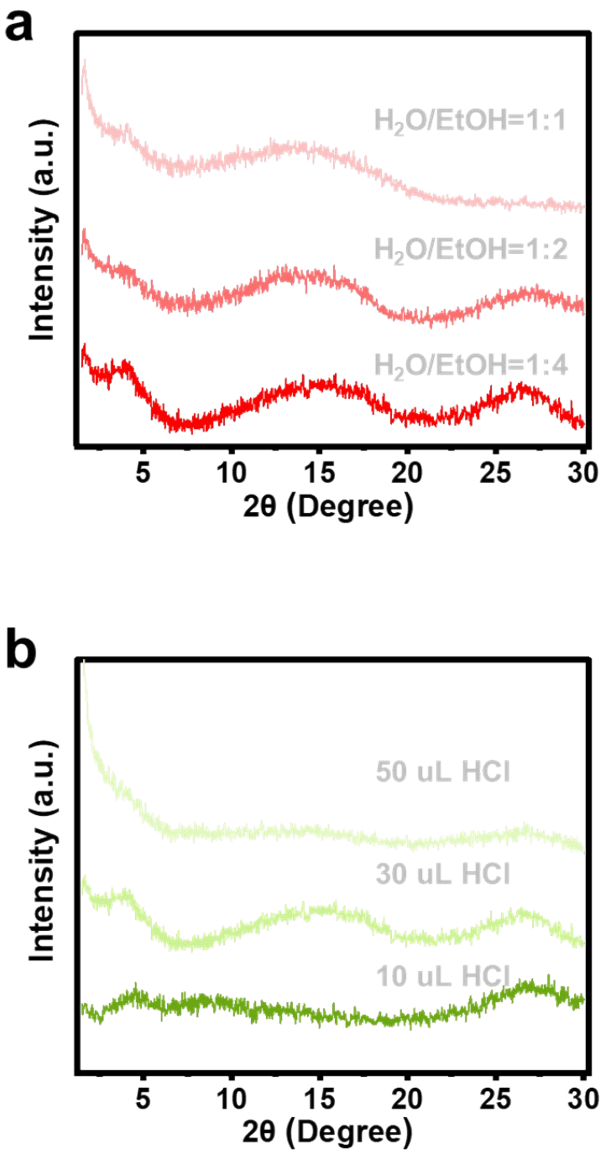

Figure S1. Crystallinity optimization experiments of PV. a) The influence of water: EtOH ratio on PV crystallinity, with the highest crystallinity observed at a water:EtOH ratio of 1:4. b) The influence of acidity, with optimal HCl addition amount of 30 μL.

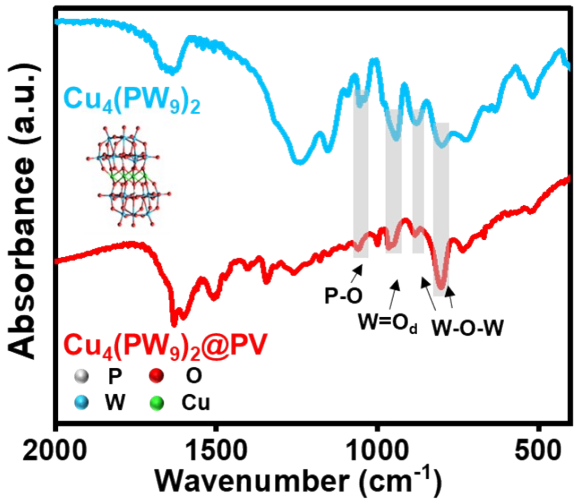

Figure S2. FT-IR comparison of $Cu_4(PW_9)_2$ and $Cu_4(PW_9)_2$@PV.

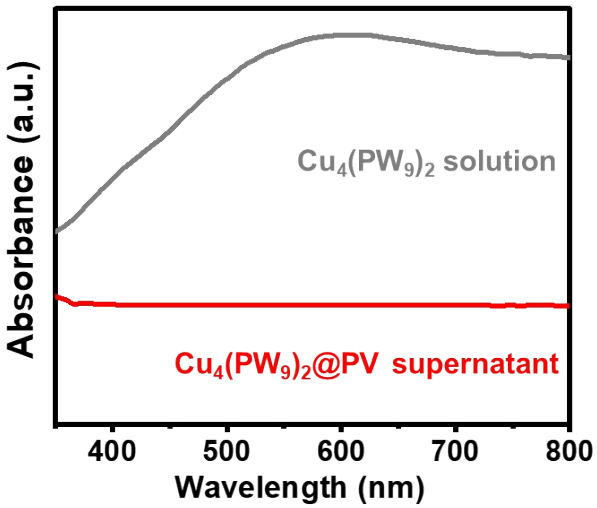

Figure S3. UV-Visible spectra of $Cu_4(PW_9)$ aqueous solution and the solution immersing $Cu_4(PW_9)_2$@PV at 50 ℃ for 6 h.

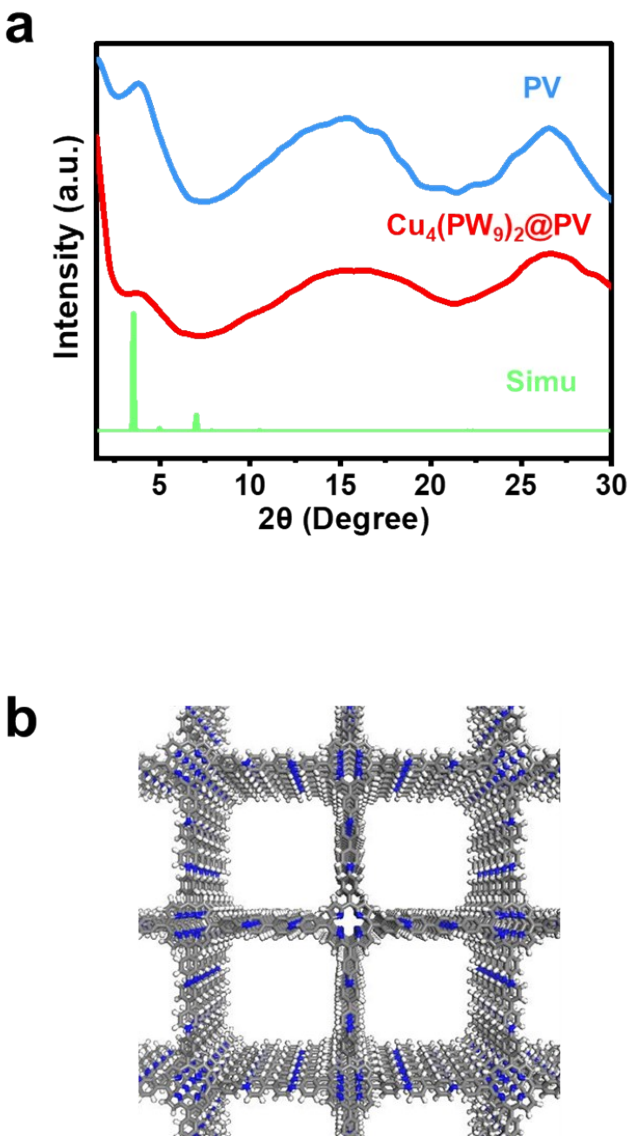

Figure S4. a) PXRD patterns of PV, $Cu_4(PW_9)_2$@PV and simulated PXRD pattern of PV. b) AA stacking model image of PV.

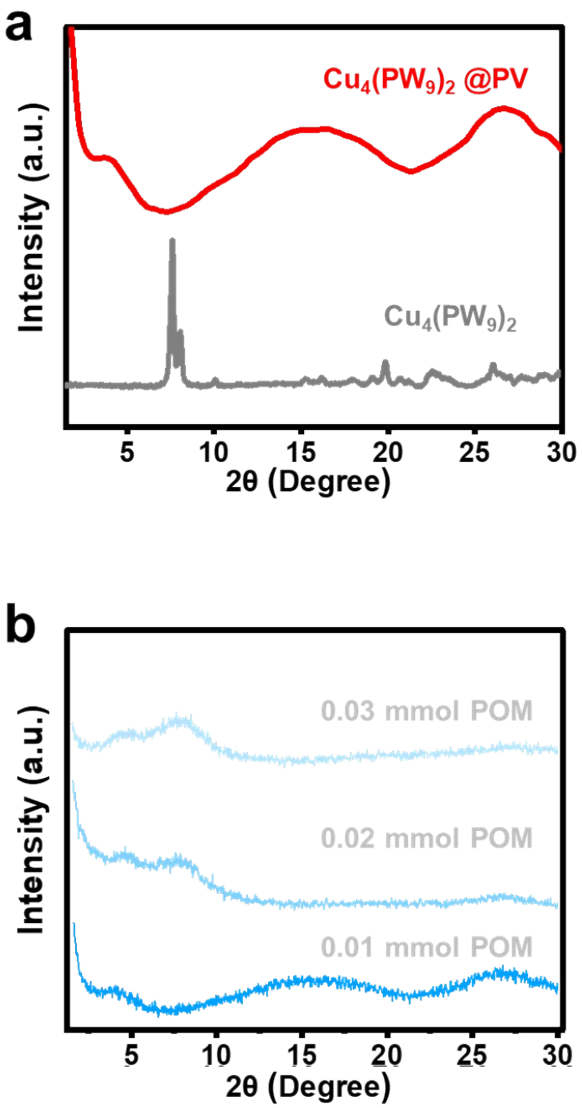

Figure S5. a) PXRD comparison of $Cu_4(PW_9)_2$ and $Cu_4(PW_9)_2$@PV. b) PXRD of $Cu_4(PW_9)_2$@PV obtained by treating with aqueous solutions containing different amount of POM.

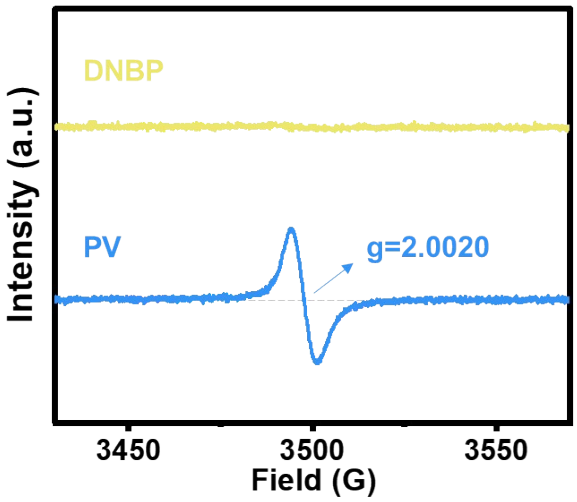

Figure S6. EPR of PV and viologen monomer DNBP.

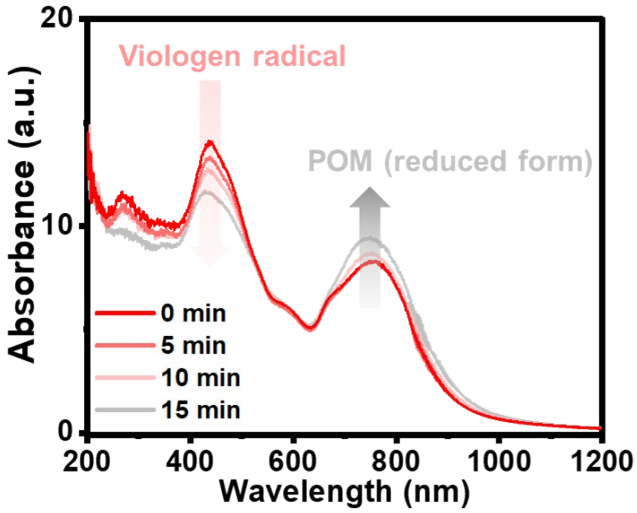

Figure S7. UV-Vis spectra of POM@PV with different Xe lamp irradiation durations.

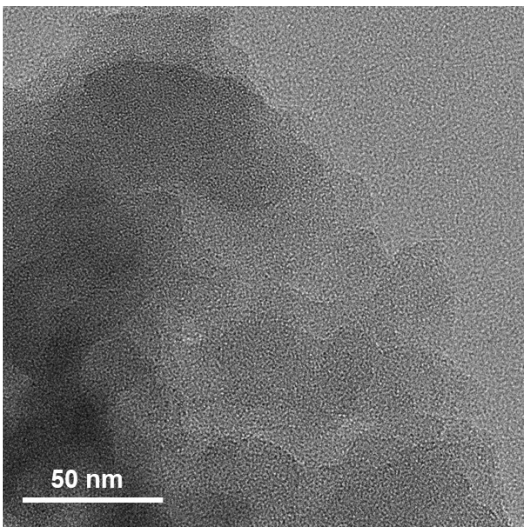

Figure S8. Transmission Electron Microscope (TEM) image of $Cu_4(PW_9)_2$@PV.

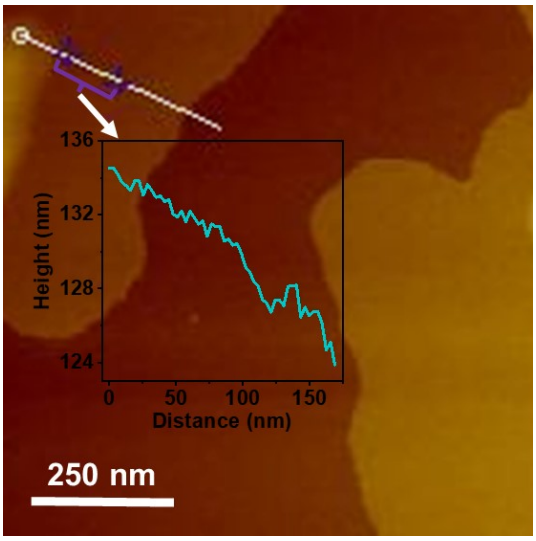

Figure S9. Atom Force Microscope image of $Cu_4(PW_9)_2$@PV.

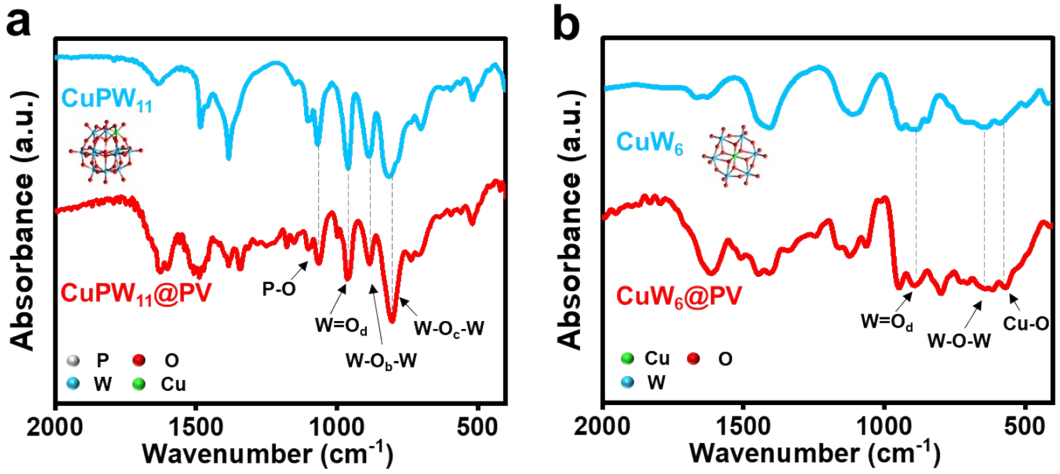

Figure S10. FT-IR of a) $CuPW_{11}$@PV, b) CuW_6@PV.

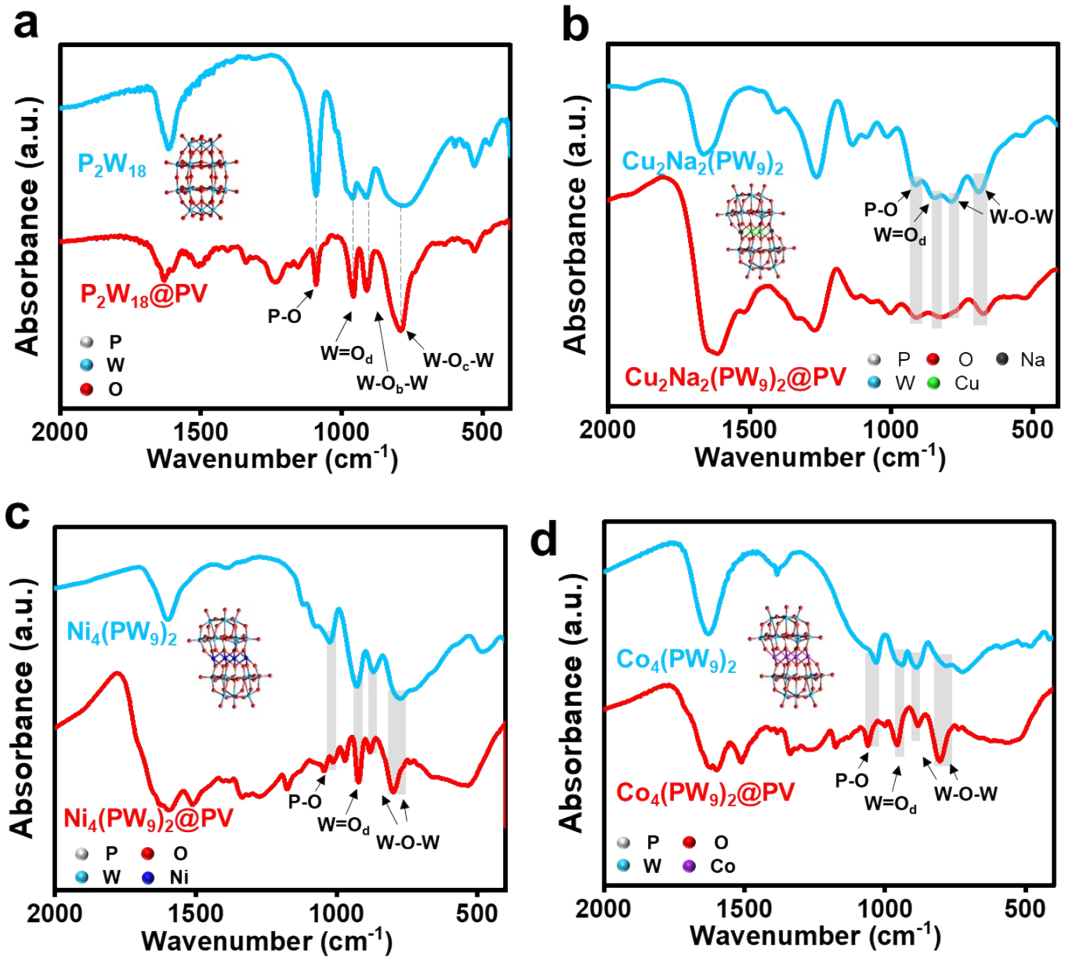

Figure S11. FT-IR of a) P_2W_{18}@PV, b) $Cu_2Na_2(PW_9)_2$@PV, c) $Ni_4(PW_9)_2$@PV, d) $Co_4(PW_9)_2$@PV.

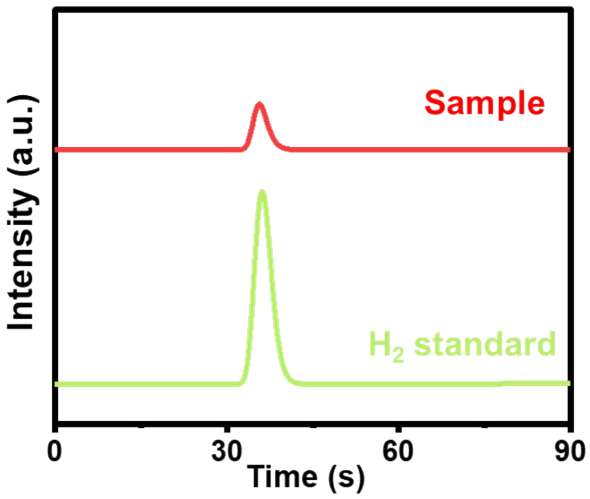

Figure S12. GC chromatogram of headspace gas above the cathode solution after reaction (red, sample) and H_2 standard sample (green).

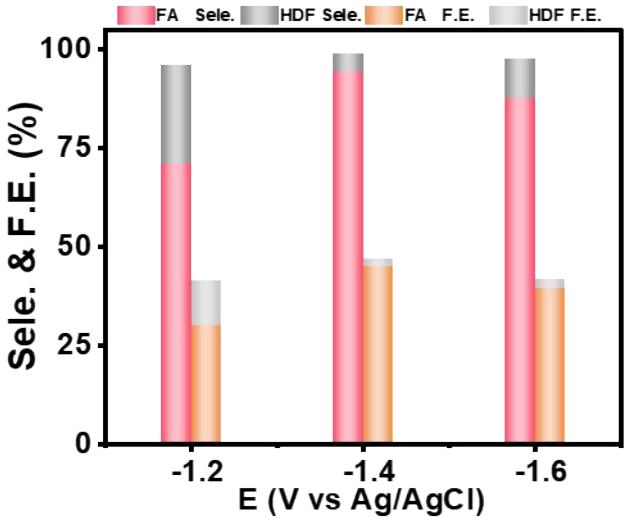

Figure S13. Electroreduction of FF over $Cu_4(PW_9)_2$@PV at different applied potentials.

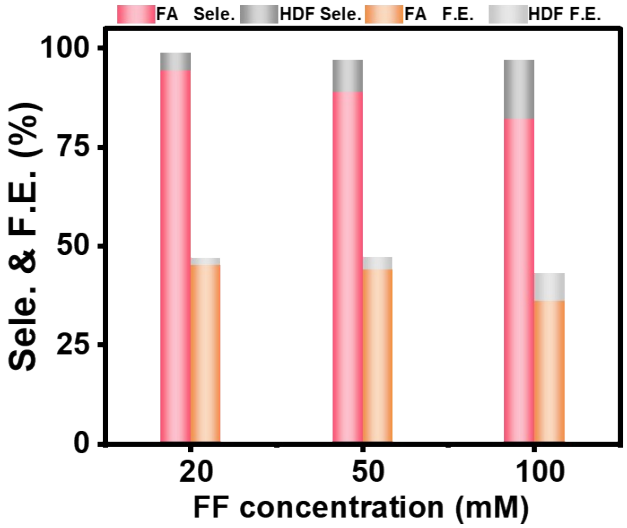

Figure S14. Electroreduction experiments of FF at different FF concentration.

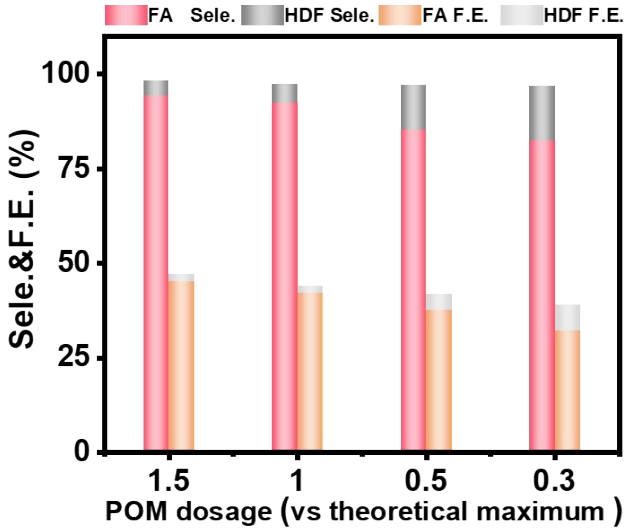

Figure S15. Electroreduction experiments of FF over $Cu_4(PW_9)_2$@PV from different POM dosages.

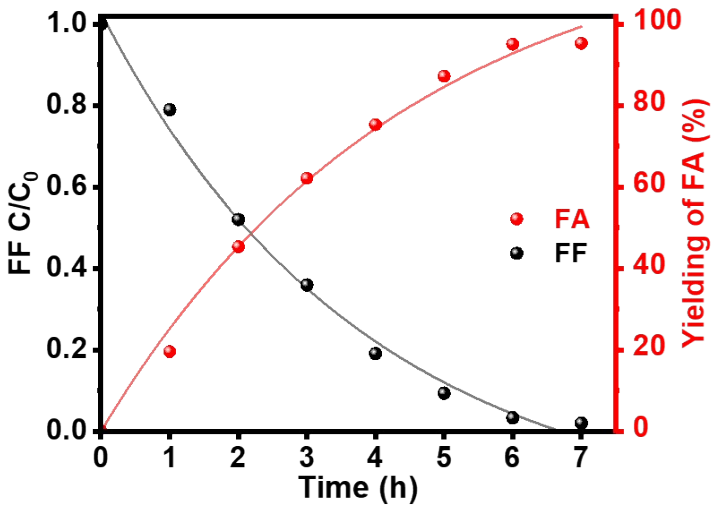

Figure S16. Electroreduction of FF over $Cu_4(PW_9)_2$@PV in 7 hours.

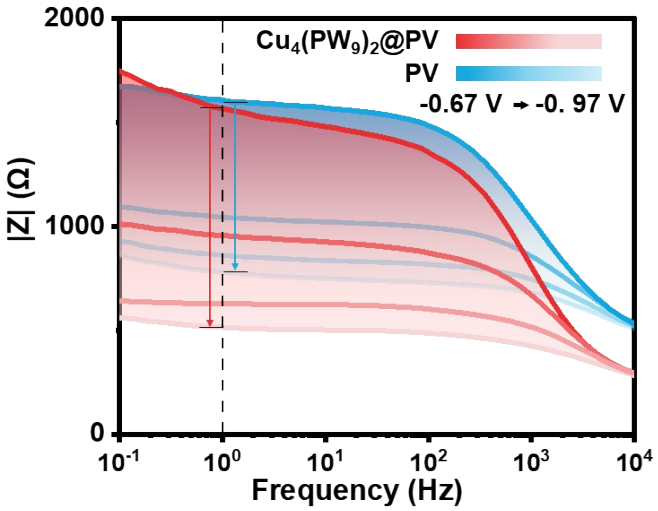

Figure S17. |Z|-frequency Bode plot of PV and $Cu_4(PW_9)_2$@PV at increasing applied potential.

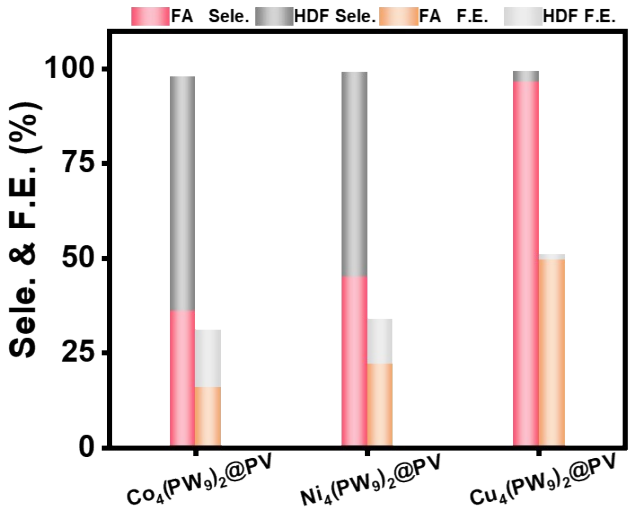

Figure S18. Electroreduction of FF over $M_4(PW_9)_2$@PV (M=Cu, Co, Ni).

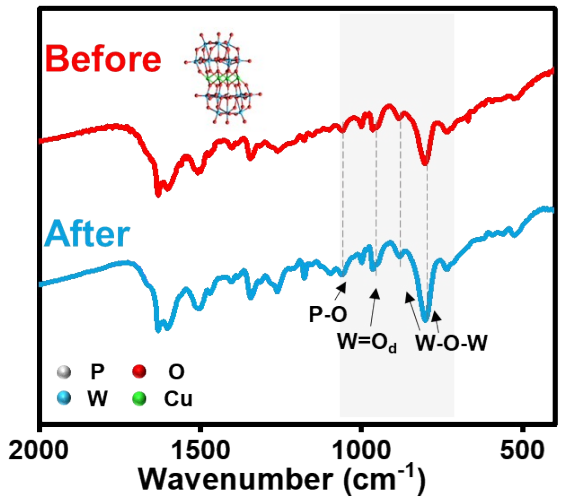

Figure S19. FT-IR spectra of $Cu_4(PW_9)_2$@PV before electrolysis and after 3 cycles.

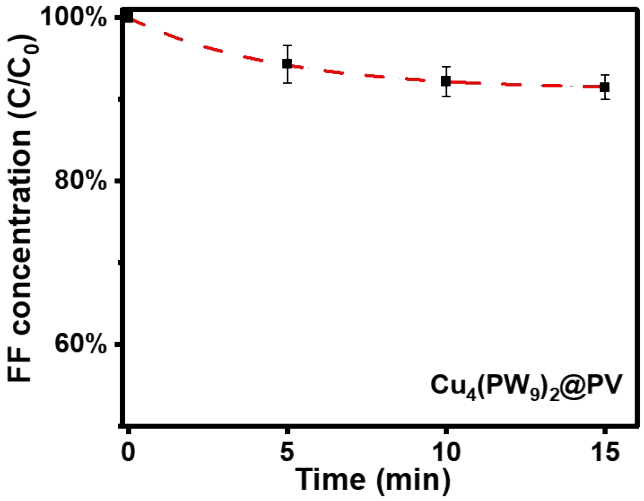

Figure S20. Adsorption of FF on $Cu_4(PW_9)_2$@PV.

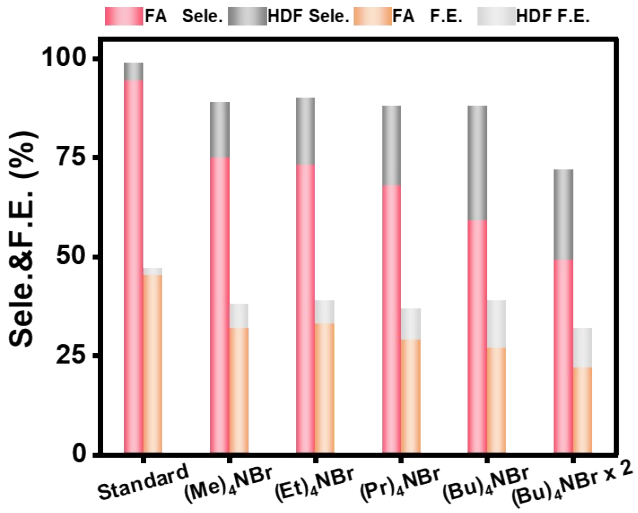

Figure S21. Influence of quaternary alkyl ammonium cations on electroreduction of FF to FA over $Cu_4(PW_9)_2$@PV.

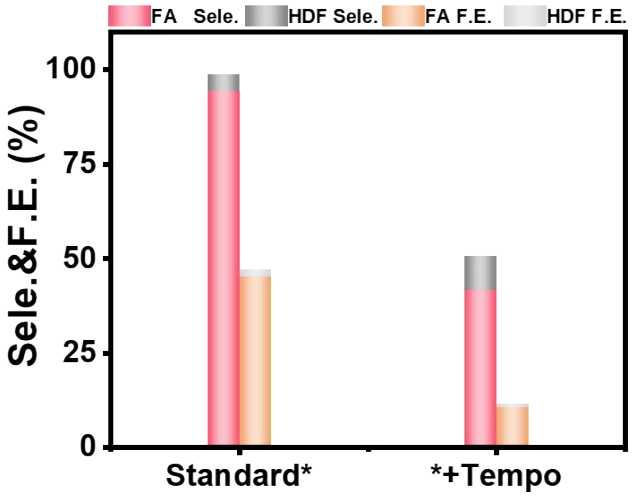

Figure S22. Electroreduction of FF over $Cu_4(PW_9)_2$@PV with radical scavenger.

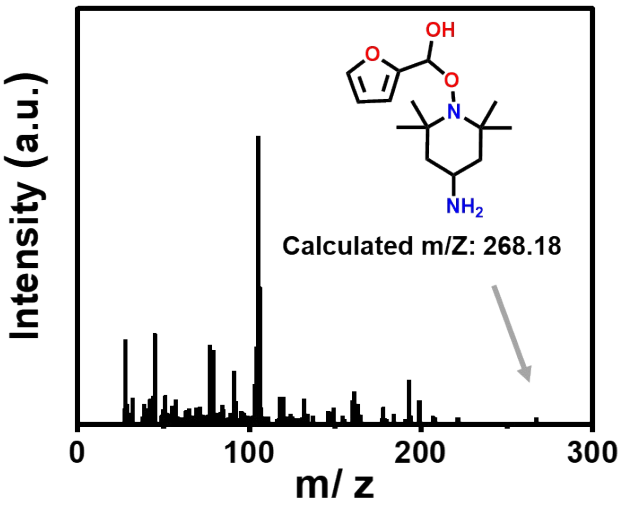

Figure S23. GC-MS chromatogram of intermediate-TEMPO adduct.

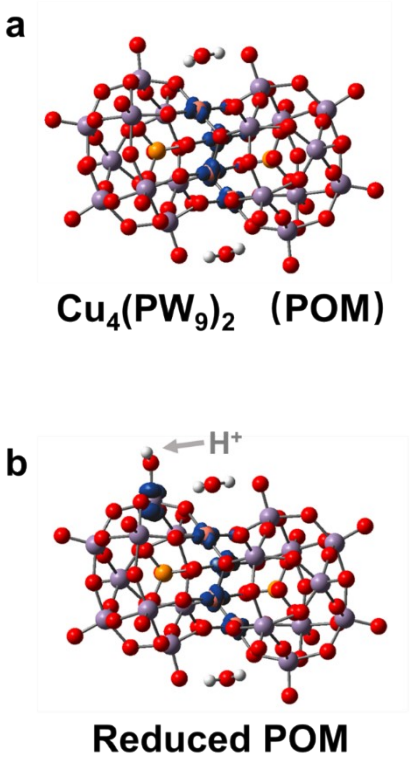

Figure S24. Spin density plots of a) $Cu_4(PW_9)_2$, b) reduced $Cu_4(PW_9)_2$ with a combined proton. Isovalue was set as 0.05 e $Å^{-3}$.

References

1 O. Buyukcakir, S. H. Je, S. N. Talapaneni, D. Kim and A. Coskun, *ACS Applied Materials & Interfaces*, 2017, **9**, 7209-7216.

2 H. Lv, W. Guo, K. Wu, Z. Chen, J. Bacsa, D. G. Musaev, Y. V. Geletii, S. M. Lauinger, T. Lian and C. L. Hill, *Journal of the American Chemical Society*, 2014, **136**, 14015-14018.

3 J. W. Vickers, H. Lv, J. M. Sumliner, G. Zhu, Z. Luo, D. G. Musaev, Y. V. Geletii and C. L. Hill, *Journal of the American Chemical Society*, 2013, **135**, 14110-14118.

4 H. Lv, Y. Gao, W. Guo, S. M. Lauinger, Y. Chi, J. Bacsa, K. P. Sullivan, M. Wieliczko, D. G. Musaev and C. L. Hill, *Inorganic Chemistry*, 2016, **55**, 6750-6758.

5 Y. Hou, L. Xu, M. Cichon, S. Lense, K. Hardcastle and C. Hill, *Inorganic Chemistry*, 2010, **49**, 4125-4132.

6 J. Zhang, D. Shi, J. Yang, L. Duan, P. Zhang, M. Gao, J. He, Y. Gu, K. Lan, J. Zhang, J. Liu, D. Zhao and Y. Ma, *Advanced Materials*, 2024, **36**, 2409188.

7 P. Gouzerh and A. Proust, *Chemical Reviews*, 1998, **98**, 77-112.